The impact of a Southern Ocean cyclonic eddy on mesopelagic micronekton

Alice Della Penna[1,2], Joan Llort[3], Sebastien Moreau[4], Ramkrushnbhai Patel[5,6], Rudy Kloser[7], Peter Gaube[8], Peter Strutton[5], Philip Boyd[5];

1. Institute of Marine Science, University of Auckland, New Zealand
2. School of Biological Sciences, University of Auckland, New Zealand
3. Barcelona Supercomputing Center, Barcelona, Spain
4. Norwegian Polar Institute, Fram Center, Tromsø, Norway
5. Institute for Marine and Antarctic Studies (IMAS), University of Tasmania (UTas), Hobart, Tasmania, Australia
6. Australian Research Council Centre of Excellence for Climate System Science, University of Tasmania, Hobart, Tasmania, Australia
7. CSIRO Oceans and Atmosphere, GPO Box 1538, Hobart, Tasmania, 7001, Australia
8. Applied Physics Laboratory, University of Washington, Seattle, Washington, United States of America

Corresponding author: Alice Della Penna (alice.dellapenna@gmail.com)

Key Points:

- We observed the distribution of Deep Scattering Layers (DSL) in the mesopelagic across a Southern Ocean cyclonic eddy.
- Acoustic properties such as integrated backscattering and DSL distribution within the cyclonic eddy were similar to its origin waters.
- The eddy presented a unique habitat compared to its surrounding waters, affecting the accessibility of mesopelagic prey to diving predators.

Abstract

Southern Ocean eddies shape the foraging ecology of marine apex predators such as marine mammals and seabirds. A growing number of animal tracking studies show that predators alter their swimming, diving, and foraging behavior in mesoscale eddies. However, little is known about how Southern Ocean eddies influence the distribution of mesopelagic micronekton (fish, squid, and crustaceans), which are major prey items of megafauna. Studies in other parts of the world have found that eddies can impact the abundance and community composition of micronekton. Here, we analyze acoustic observations from a 14-day survey of a mesoscale eddy, its surrounding waters, and the Sub-Antarctic frontal waters where the eddy originated. We report and interpret spatial patterns of acoustic backscattering at 18 kHz, a proxy indicating combined changes in species, size, and abundance of micronekton. We find that the vertical distribution of Deep Scattering Layers matched the underwater light conditions characteristic of the eddy core, periphery, and surrounding waters, at scales smaller than 10 km. Furthermore, the average water-column integrated acoustic backscattering values in the eddy core were only half of the values measured in the Sub-Antarctic Zone waters surrounding the eddy. By contrast, the acoustic properties of the eddy core were similar to those measured in the Polar Front Zone, where the eddy originated 27 days before our sampling. These results show that, as for physical

42   and chemical tracers, the eddy maintained its biological characteristics from its source waters
43   creating a unique habitat compared to its surrounding waters.
44

45   **Plain language summary**

46   Mesoscale eddies are rotating currents that are ubiquitous in the ocean. They are the oceanic
47   equivalent of weather patterns and have typically radii of 10-100 km and lifetimes between
48   weeks and months. Mesoscale eddies have a dramatic impact on the distribution of primary
49   production in the open ocean, on the transport of heat and salt across oceanic regions, on global
50   biogeochemical cycles, and on the feeding behavior of apex predators such as pinnipeds, sharks,
51   billfishes, and seabirds. In this study, we evaluated the impact of a Southern Ocean mesoscale
52   eddy on the distribution of deep water micronekton, a diverse group of small animals including
53   fish, crustacea, and squids. We found that the abundance and vertical distribution of deep water
54   micronekton, detected using a sonar, inside the sampled mesoscale eddy differed from those of
55   the surrounding waters. Micronekton distribution and abundance were instead more similar to
56   those of the locations where the eddy had originated a month prior to our sampling. Our results
57   suggest that mesoscale eddies can maintain their biological characteristics from its source waters
58   creating a unique habitat compared to its surrounding waters.

59

60   **1 Introduction**

61   Southern Ocean mesoscale eddies, rotating currents characterized by spatio-temporal scales of
62   10-100 km and lifetimes weeks-months, are key foraging regions for top marine predators such
63   as mammals (Campagna et al., 2006; Dragon et al., 2010; Bailleul et al. 2010; Della Penna et al.,
64   2015; Cotté et al., 2015) and seabirds (Cotté et al., 2007). These animals forage primarily on
65   micronekton, including small fish, cephalopods and crustaceans, and mesozooplankton, which
66   mostly inhabit the mesopelagic zone (the stratum lying between 200 and 1000 m depth;
67   McMahon et al., 2019).

68

69   Despite their importance for marine ecosystems (Murphy et al., 2016; Subramanian et al., 2020),
70   little is known about mesopelagic micronekton and how mesoscale eddies may affect their
71   distribution. These organisms are challenging to observe: they are too small to be tagged with the
72   animal tracking devices used to study top predators and are invisible to our current satellite
73   sensors, which are generally limited to observing the near-surface of the ocean. Current methods
74   to observe mesopelagic micronekton include mid-water trawling (Wiebe et al.,1985; Greene et
75   al. 1990), optical devices (Kloser et al., 2016) and acoustic methods (Kloser et al., 2009; Ryan et
76   al., 2009). Furthermore, micronekton varies at many temporal and spatial scales. These include
77   the scales spanning diel vertical migration behavior (DVM; Cuvier, 1817; Hays, 2003) to
78   seasonal and inter-annual variability (Urmy et al.,2016; Escobar-Flores et al., 2018).
79   Disentangling this variability in the remote Southern Ocean is further complicated by the
80   logistical challenges of collecting ship-based data in the often harsh conditions of this region.
81
82
83   In recent years, the number of observations of acoustic backscattering has been growing,
84   resulting in the creation of datasets of multi-frequency observations from research vessels and
85   ships of opportunity (Kunnath et al., 2021). These new observations facilitate an analysis of the

86 spatial distribution of biogeographical provinces, or bio-regions, for mesopelagic organisms
87 (*e.g.*, Proud et al. 2015; Klevjer et al. 2016). Bio-regions define the large-scale habitat of the
88 marine animals that prey on mesopelagic nekton. Yet, such bio-regions do not capture the fine-
89 scale variability that highly mobile predators encounter during their foraging trips. This
90 variability is largely influenced by mesoscale and submesoscale features such as fronts,
91 filaments, and eddies (Tew-Kai et al., 2009; Bost et al., 2009; Gaube et al., 2018; Braun et al.,
92 2019; Chapman et al., 2020) and is central in understanding the role of patchiness in modulating
93 biogeochemical fluxes (Moreau et al., 2017; Frenger et al, 2018; Orselli et al., 2019; Rohr et al.,
94 2020a-b, Patel et al., 2020). An improved understanding of how fine scales distribute
95 micronekton and mesozooplankton (the so-called *intermediate trophic levels*) is pivotal for
96 building a comprehensive view of marine ecosystems, from phytoplankton all the way to top
97 predators, as well as their role on exporting carbon into the deep ocean (Belcher et al, 2019,
98 Davison et al, 2013).
99
100 In the North Atlantic, a handful of studies observed how eddies impact the distribution of
101 micronekton using both midwater trawls and acoustic backscattering (Boyd et al. 1986;
102 Craddock et al., 1992; Godø et al., 2012; Fennel and Rose, 2015; Della Penna and Gaube, 2020;
103 Devine et al., 2021). In this region, eddies differed in micronekton abundances, community
104 composition and patterns in acoustic backscattering from their surrounding waters. A growing
105 number of studies are addressing the distribution of acoustic backscattering in the Southern
106 Ocean, either to relate observed patterns to hydrographic features (Behagle et al., 2017; Escobar-
107 Flores et al. 2018) or to define the boundaries of mesopelagic biogeographies (Proud et al.,
108 2015). However, to our knowledge, no study has explicitly addressed how Southern Ocean
109 mesoscale eddies affect the distribution of acoustic backscattering associated with micronekton.
110
111 Here, we combine hydrographical and acoustic measurements to analyze how a Southern Ocean
112 cyclonic eddy affected acoustic backscattering vertically integrated over the upper 1,200 m, as
113 well as its impact on the distribution of DSL. First, we highlight the contrasting distributions of
114 DSL inside the eddy core with the surrounding waters from the case study of a transect. We
115 relate some of these differences with gradients in the underwater light field and light attenuation
116 properties in the water column. Second, we show how the integrated distribution of acoustic
117 backscattering in the water column within the eddy core relates to ambient SAZ waters and the
118 waters in the PFZ where the eddy formed. Finally, we discuss how the provenance of the eddy
119 influences the resident micronekton. Specifically, while the eddy core displays micronekton
120 acoustical properties that are more similar to its origin, the waters at the eddy periphery display
121 more similarities to the SAZ, suggesting that the resident mesopelagic communities are mixed –
122 at the eddy margins - with those from the SAZ.

2 Materials and Methods

123
124 *2.1 Multi-platform sampling of the eddy and its region*
125 The studied Southern Ocean cyclonic feature was tracked using satellite data (altimetry-derived
126 Sea Surface Height and Sea Level Anomaly (SLA), Sea Surface Temperature, and near-surface
127 chlorophyll) and sampled during the voyage IN2016_V02 of the Australian *RV Investigator*
128 (Patel et al., 2019). In particular, we used SLA maps to track and illustrate the position and shape
129 of the eddy (Fig.1). SLA data were downloaded from the Copernicus CMEMS web portal as
130 daily maps gridded to a nominal spatial resolution of ¼°. The studied eddy had been first

131   identified as a meander in the Sub-Antarctic Front (SAF) on 3 February 2016 that then detached
132   as a cyclonic eddy and started moving northward on 3 March 2016 (Patel et al., 2019). The eddy
133   had a diameter of approximately 190 km and was sampled between the 30 March and 5 April
134   2016, approximately 20 days before the eddy was re-absorbed by a SAF meander.

135   After sampling the eddy with a star-shaped pattern of Conductivity-Temperature-Depth (CTD)
136   stations (Fig. 1), the *RV Investigator* headed to the PFZ, where the eddy had originated 27 days
137   before the beginning of our sampling (Moreau et al., 2017; Patel et al., 2019). The PFZ and the
138   SAF were observed for ~ 18 hours before the *RV Investigator* headed back towards port in
139   Hobart, Tasmania, allowing for some more sampling of the SAZ in the proximity of the eddy.

140   Physical, biological, biogeochemical, and acoustic measurements were performed inside the
141   eddy, in the surrounding SAZ and in the PFZ. Continuous sampling with a thermosalinograph,
142   an in-line fluorometer, and 18 CTD casts revealed a marked doming of isopycnals as well as
143   anomalies in temperature, oxygen distribution, salinity, chlorophyll and nutrients inside the eddy
144   (Moreau et al., 2017; Patel et al., 2019; Patel et al.,2020). The onboard 75 kHz acoustic Doppler
145   current profiler (ADCP) was used to identify the location of the eddy center following Patel et al.
146   (2019) and to discriminate between the eddy core and periphery (in red and ochre respectively in
147   Fig. S1). Here, we consider the eddy core as the region within 25 km from the eddy center,
148   where geostrophic velocities near the surface were smaller than 30 cm/s (Patel et. al, 2019). We
149   assume all observations within an anulus with radii of 25 km and 75 km away from the eddy
150   center as belonging to the eddy periphery. *In situ* physical and biogeochemical measurements
151   discussed by Moreau et al., (2017) were used to define the boundaries between the PFZ and the
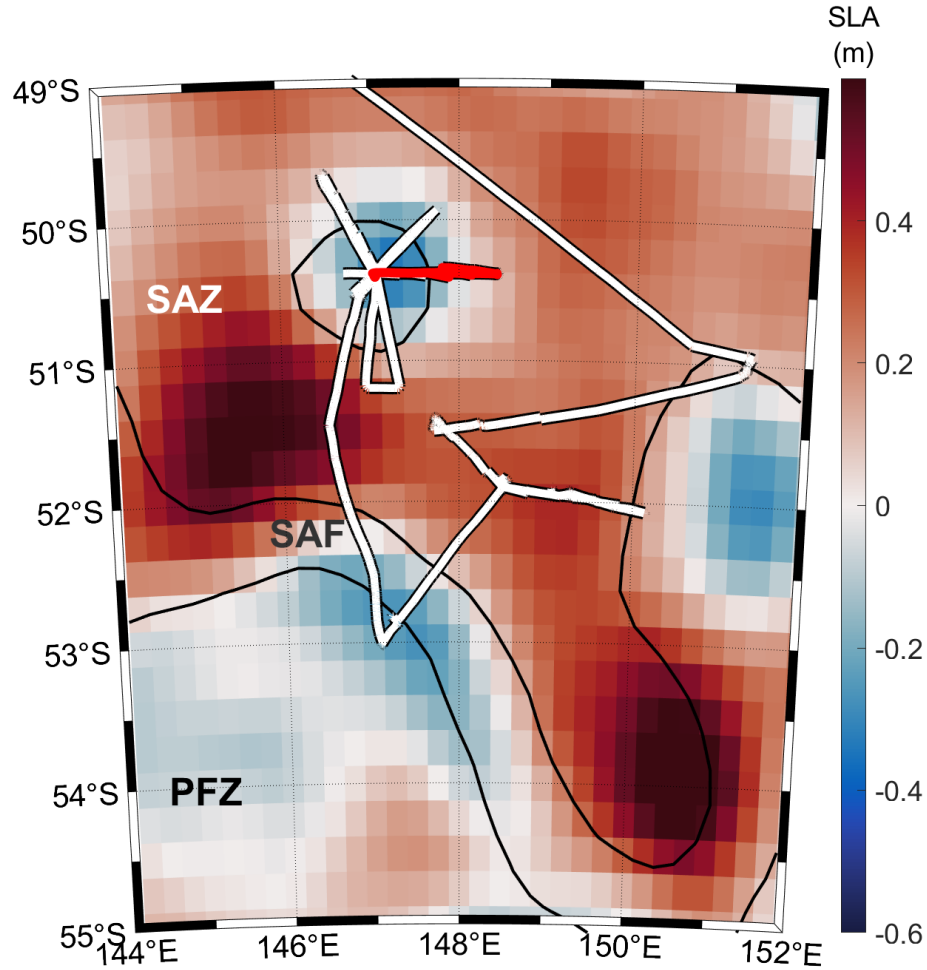152   SAZ.

153
154 **Figure 1 Map of Sea Level Anomaly (SLA, referring to 01/04/2016) for the region of interest.**
155 *Black contours indicate isolines of Sea Surface Height and identify the eddy and two branches of*
156 *the Sub-Antarctic Front (SAF). White lines identify the ship track. The transect shown in Figure*
157 *2 corresponds to the part of the ship track marked in red.*

158
159
160

161 *2.2 Acoustic measurements and processing*
162 A single-beam scientific echosounder (*Simrad EK60, Kongsberg Maritime*) was used to measure
163 acoustic volume backscattering (Sv dB re 1 m^{-1}) during the entire duration of the trip at the
164 frequency of 18 kHz. Pulse length and pinging period were 2 ms and 0.2 Hz respectively. The
165 echosounder was calibrated prior to the voyage and we assume no change in the Sv calibration
166 with surface temperature as sound velocity induced variations cancel out (Bodholt, 2002). Since
167 our study is focused on comparing patterns in the distribution of Sv, any bulk echosounder
168 performance change should not impair the analysis of the gradients we present. In total, we
169 collected more than 308 hours of acoustic data, 159 during daytime and 149 during night-time:
170 62 hours inside the eddy core (42 daytime/20 night-time), 55 hours within the periphery of the
171 eddy (23/32), 173 hours in the SAZ (82/91) and 18 hours in the PFZ and SAF (12/6, Table 1).

172   Daytime and night-time observations were classified by comparing the time-stamp associated
173   with each ping with the sunrise and sunset times computed for the associated longitude and
174   latitude calculated using the equations described in Meus et al., (1991). Observations collected
175   within 30 minutes of sunrise and sunset were excluded for the average daytime or night-time
176   profiles and only retained to plot the echograms (Bianchi and Mislan, 2016). Raw data of
177   backscattered power were processed using ESP3, an open-source software, Matlab-based
178   package for visualizing and processing acoustics data, developed by the deepwater fisheries
179   acoustics team at NIWA (Wellington, New Zealand, https://sourceforge.net/projects/esp3/,
180   Ladroit et al., 2020). We assumed a sound speed of 1500 m/s and an absorption coefficient of
181   0.0027 m^{-1}. Data were processed using the software bad data detection, spike detection, and
182   noise filtering algorithms (with a noise threshold of -140 dB, spike threshold of 10 dB). No
183   corrections were made for non-linear power responses as outlined by De Robertis et al., (2019)
184   as our results are treated as relative indicators and were not used to calculate fish biomass.
185   Observations from depths below 1,200 m and shallower than 15 m were excluded from this
186   analysis since the corresponding signal tends to be dominated by noise or the waves and bubbles
187   near the surface. Nautical area scattering coefficients (NASC) were calculated using the
188   equations detailed in MacLennan, (2002) over depth intervals of 5m. NASC is commonly used in
189   fisheries acoustics to represent the linear increase in the numbers of biomass of fish present of
190   similar size/weight and acoustic reflectivity.
191
192

	Eddy core	**Eddy periphery**	**SAZ**	**PFZ**
Daytime	40	23	82	12
Night-time	20	32	91	6
Total	62	55	173	18

193   ***Table 1: Duration of sampling*** *in hours for the different subregions explored during*
194   *IN2016_V02*
195
196
197   *2.3 Estimates of underwater light-levels and near-surface fluorescence*
198   We used vertical profiles of photosynthetically available radiation (PAR) to estimate the vertical
199   distribution of irradiance and describe the light levels encountered by the mesopelagic organisms
200   in the different sampled subregions. Daytime CTD casts with PAR measurements were obtained
201   from the subregions as follows: 4 in the eddy core, 4 at the periphery, 3 in the SAZ and 2 in the
202   PFZ. Since the light levels that characterize the mesopelagic are below the detection limit of the
203   PAR sensor (Log Quantum Cosine Irradiance Sensor, QCP2300, Biospherical), we estimated a
204   representative coefficient of diffuse light attenuation, k_d(PAR), for each subregion. Daytime
205   observations of PAR between 50-180m were used to fit a linear relationship between log(PAR)
206   and depth (Fig. S2 in the Supplementary Materials). These k_d(PAR) values were used to estimate
207   the average profiles of irradiance for each subregion and compared using a Student's *t* test.
208
209   In the transition between subregions, we used uncalibrated measurements of fluorescence of
210   near-surface water sampled through the shipboard flow-through system using a WETStar
211   fluorometer (WS3S-443P, Wetlabs, SeaBird Inc.). As detailed in Moreau et al., (2017), these
212   fluorescence measurements were impacted by differences in the fluorescence yield per unit

213 chlorophyll during different times of the day. However, the observations still produced a
214 meaningful and consistent quantification of near-surface chlorophyll. We chose to use
215 fluorescence to identify the strong gradient in near-surface chlorophyll associated with the
216 periphery of the sampled eddy.
217
218 *2.4 Historical acoustics observations of the Southern Ocean*
219 To provide context for our acoustics observations, we integrated into our study a collection of
220 acoustic observations collected by research vessels and ships of opportunity from the Integrated
221 Marine Observing System (IMOS) / Australian Ocean Data Network (AODN,
222 https://portal.aodn.org.au/). This dataset contains processed acoustic backscattering (S_v) that has
223 been filtered for different types of noise following the guidelines described in Kunnath et al.
224 (2021). From this relatively large dataset, we selected only the observations collected at 18 kHz
225 during the summer-fall months (January-May), which restricted the dataset to ten voyages and
226 corresponded to more than 700 hours of sampling (Table S1, Fig. S4). We then separated the
227 observations obtained in the SAZ from the ones collected south of the SAF (in the PFZ). The
228 SAF was defined using the 0.2 m isoline of Sea Surface Height following Sokolov and Rintoul
229 (2009). To homogenize the sampling frequencies for the voyages, all acoustics observations were
230 interpolated at 30 minutes' intervals.
231

3 Results

233 The vertical distribution of DSL inside the eddy core were remarkably different compared to the
234 surrounding SAZ waters (Fig.2). The example in Fig.2 showcases observations of acoustic
235 backscattering sampled while the *RV Investigator* was transiting from the core of the eddy to the
236 ambient SAZ waters. As the vessel's distance from the eddy center approached 25 km (blue line
237 in Fig. 2b), patterns in the distribution of acoustic backscattering changed dramatically (~3:00
238 a.m. UTC/ 13:00 local time, white dashed line in Fig. 2a and black line in Fig. 2b).
239
240 The depths of several DSL that are present both inside the eddy core and at the periphery were
241 remarkably different in these two subregions (Fig. 2a). For instance, the deepest scattering layer
242 in the core shoaled from ~ 1200m to 900m as the distance from the center increased, while the
243 lower limit of the non-migrating DSL became ~ 100 m shallower. The upper limit of the non-
244 migrating DSL also moved up in the water column as the ship transited outside of the eddy core.
245 The general movement of all DSLs towards shallower depths correlated with the uplift of
246 isolumes (depths characterized by the same light levels, dotted black lines in Fig. 2a). The latter
247 was in turn linked to higher surface chlorophyll outside the eddy, which enhanced light's
248 attenuation and reduced light's penetration into the water column (Fig. 2b). Light attenuation
249 coefficients in the eddy core were significantly different from those of the eddy periphery
250 ($p<0.05$), and surrounding SAZ waters ($p<0.05$), yet not significantly different ($p=0.07$) from the
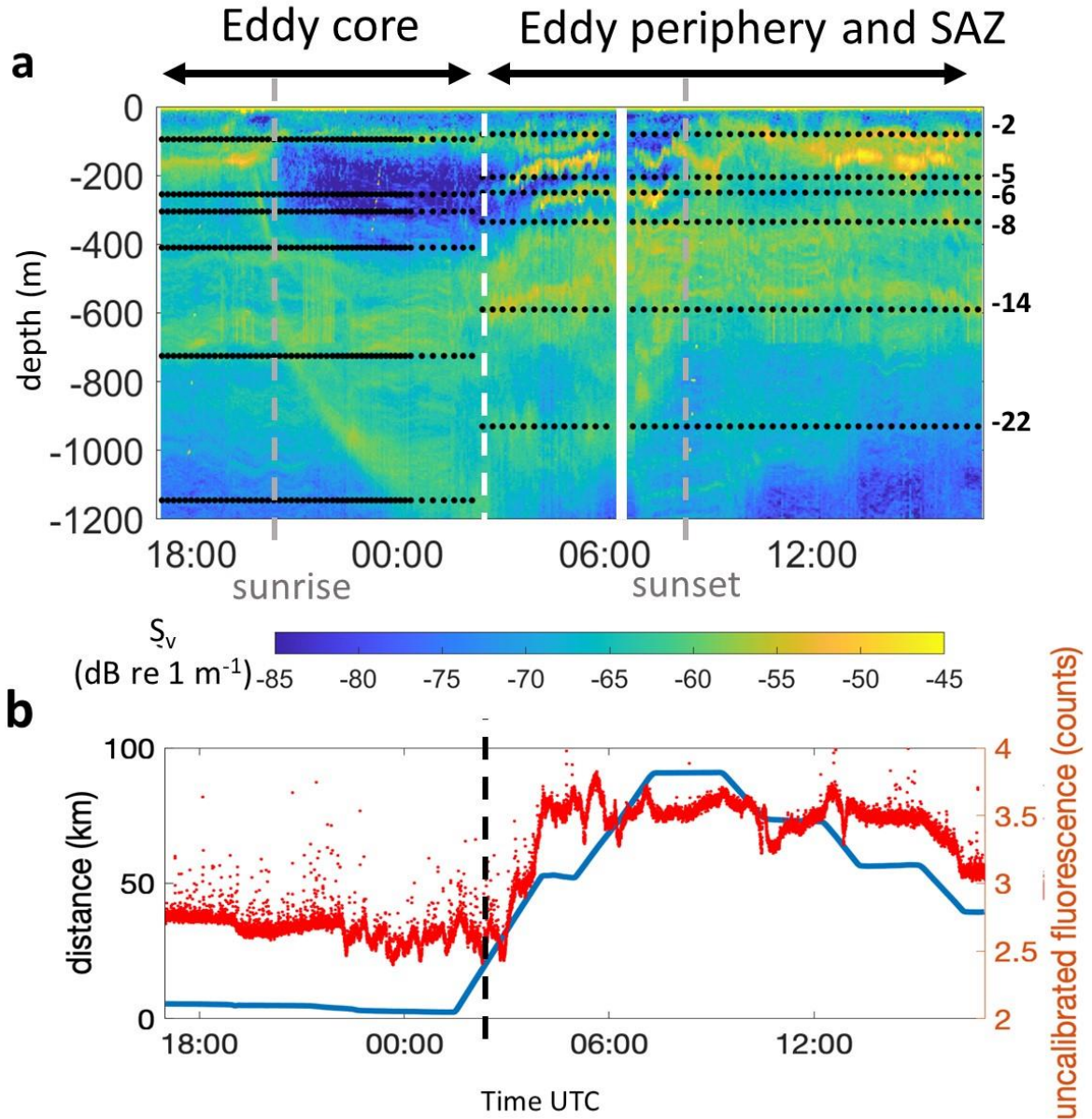251 origin PFZ waters (Fig. S3).
252
253

254
255

256 ***Figure 2 Echogram (a) showcasing an example of transition between eddy core (18:00-03:00***
257 ***UTC / 04:00-13:00 local time) and eddy periphery (03:00-16:00 UTC / 13:00-02:00 local time).***
258 *This echogram refers to the time starting on 31/03/2016 UTC. Grey vertical dashed lines*
259 *indicate the times corresponding to the DVM (towards and from the mesopelagic from left to*
260 *right at approximately 20:00 UTC/ 06:00 local time and 08:00 UTC/18:00 local time,*
261 *respectively) and the white dashed line represents the boundary between eddy core and*
262 *periphery. White filled lines indicate data that was not retained during quality control.*
263 *Horizontal dash lines represent the position of the isolumes for the eddy core and eddy periphery*
264 *calculated from the CTD casts conducted in the respective regions. Different labeled isolumes*
265 *represent how much of the light available near the surface penetrates to a given depth, in log10*
266 *scale.. As the distance from the eddy center increases (b, blue line), the boundary of the eddy*

267   *core is crossed around 25 km away from its center and a sharp gradient in surface fluorescence*
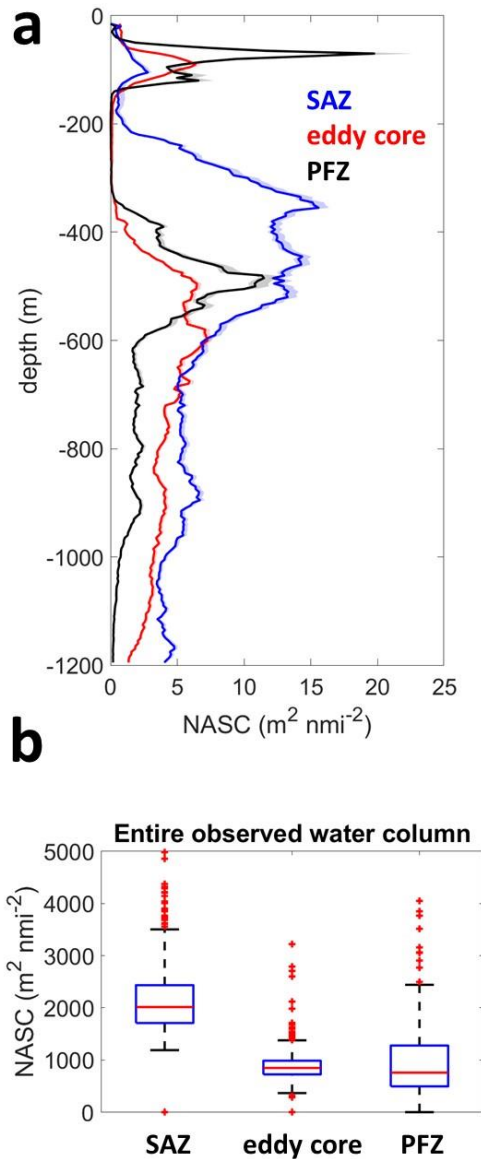268   *appears (red dots in b).*

269

270
271   ***Figure 3 Differences in the distribution of deep scattering layers (DSLs, a) and integrated***
272   ***NASC (b) between locations in the eddy core, in the Sub-Antarctic Zone (SAZ) and in the Polar***
273   *Front Zone (PFZ). Solid lines in (a) indicate the median daytime NASC values in the SAZ (blue),*
274   *in the eddy core (red), and in the PFZ (black). Shadings indicate the 25th and 75th percentiles*
275   *divided by the square root of the number of observations.*

276
277   While differences in the light field account for some of the differences between the DSLs
278   distribution in the eddy core and ambient waters, some scattering layers, such as those at 200-
279   300 m were observed immediately outside of eddy, but not inside the eddy core. In contrast, the

280   100m deep scattering layer in the eddy core was not detected at 75 km from the center of the
281   eddy.
282
283   On average, there were fewer and less acoustically reflective DSL in the eddy core compared to
284   the SAZ waters (Fig.3a, Fig. S5). The average integrated NASC inside the core of the eddy was
285   approximately 50% of the NASC in the surrounding waters of the SAZ (Fig. 3a, 3b and Fig. S6).
286   By contrast, the daytime distribution of NASC in the top 600 m (corresponding to the epipelagic
287   and upper mesopelagic) was remarkably similar to the PFZ, where the eddy had originated
288   (Fig.3a). Integrated values of NASC in the PFZ were also as low as the inside the eddy core and
289   noticeably smaller than the SAZ (Fig. 3b). This strong difference in acoustic backscattering
290   between the SAZ and the PFZ was consistently found in historical acoustic data where integrated
291   NASC values in the SAZ can be more than three times higher than in the PFZ (Fig. S4).
292
293   NASC differences between the eddy core and those in the PFZ are less than half of the
294   differences between the eddy core and the SAZ (Fig.4). Observations of NASC from the eddy
295   periphery were highly variable (ochre shading in Fig. 4,a) and, on average, intermediate between
296   the SAZ and the eddy core ones (Fig. 4a). Conversely, NASC values measured at the eddy
297   periphery are on average larger than the PFZ (positive anomalies in Fig. 4,b) throughout the
298   water column.

299

300   **4 Discussions and conclusions**

301   We examined the distribution of acoustic backscattering inside the core and at the periphery of a
302   cyclonic eddy and compared it with the typical patterns in acoustic backscattering in the SAZ
303   and in the PFZ. Our major findings, which we explore here in more detail, were as follows. First,
304   the distribution of DSL inside the eddy core was different from the ambient waters of the SAZ
305   even a month after eddy formation. Differences were partially, yet not exclusively, due to
306   changes in the light-field encountered by mesopelagic organisms due to the different horizontal
307   distribution of near-surface phytoplankton. The average water-column integrated values of
308   NASC inside the eddy core are similar to the average of the PFZ (950 m^2nmi^{-2} vs 850 m^2nmi^{-2}),
309   but lower approximately 50% of the SAZ mean (Fig. 3). Finally, the eddy periphery values of
310   acoustic backscattering were intermediate between those observed in the core and the SAZ
311   ambient waters (Fig. 4).
312
313   Inside the eddy light penetrated deeper into the water column due to low concentrations of
314   surface chlorophyll (Fig. 2b and Moreau et al., 2017). We estimated very low light attenuation
315   coefficients typical of the Southern Ocean during autumn and winter (Nelson and Smith, 1991;
316   Son and Wang, 2015). We did find statistically significant differences in light attenuation
317   coefficients between the eddy core and the PFZ (low chlorophyll, clearer waters), the SAZ
318   (higher chlorophyll), and the eddy periphery (also higher chlorophyll, higher light attenuation
319   coefficient; Fig. S2). These differences affected the vertical distribution of DSL that, consistent
320   with previous studies, matched the distribution of isolumes across the water column (Røstad et
321   al., 2016, Aksnes et al., 2017). The horizontal gradients in the depths of DSL were sharp and
322   matched the gradients in near-surface fluorescence that characterized the transition between the

323   core and the ambient waters of the SAZ, similar to other ocean basins (Della Penna and Gaube,
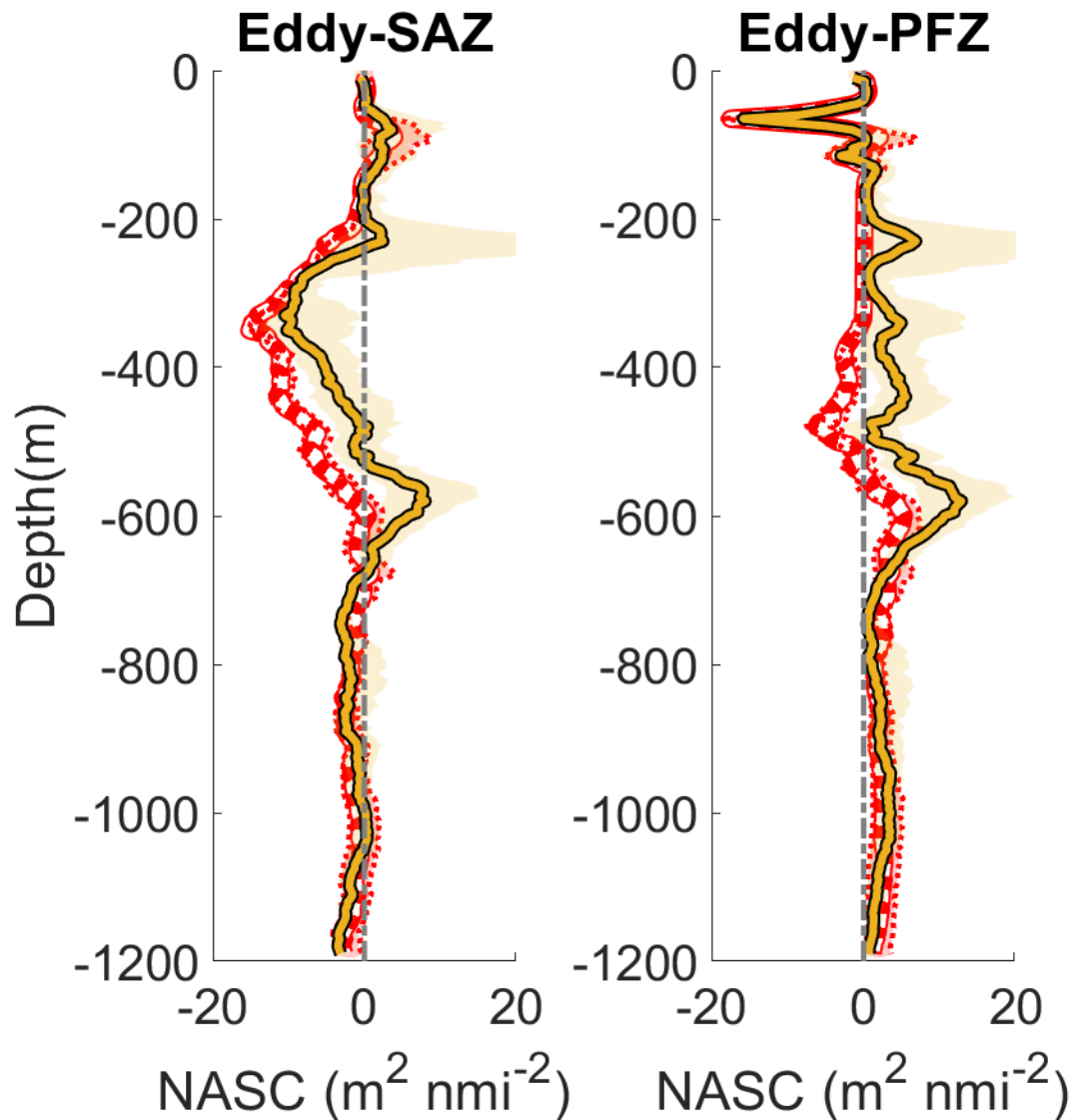324   2020).
325

326
327   *Figure 4 Differences between acoustic backscattering in selected areas of the eddy (core in*
328   *red/dashed line, periphery in yellow/ brown), the Sub Antarctic Zone (SAZ, a), and the Polar*
329   *Front Zone (PFZ, b) as a function of depth. Shadings refer to the 25th-75th percentiles of the*
330   *differences between the profiles from the eddy core and periphery compared to the median*
331   *profiles of the SAZ and PFZ respectively.*

332
333

334   We observed a different number of DSL in the eddy core, with a deeper vertical distribution
335   compared to ambient waters. Indeed, the distribution was more similar to the PFZ where the
336   eddy originated. In particular, the eddy core retained some acoustic properties typical of its
337   origin suggesting that micronekton were transported from the PFZ more than 200 km north in the
338   SAZ, probably by eddy trapping. High to mid-latitude mesoscale eddies are characterized by a

339 trapping power due to their non-linearity (Early et al., 2011). Southern Ocean eddies have been
340 suggested to trap, retain, and transport water parcels inside their cores (d'Ovidio et al., 2013).
341 Our eddy had rotational speed averages of ~40 km/day and a translational speed between 1.5-6.6
342 km/day (1.7 km/day at the time of sampling, and maxima of 6.6 km/day when detaching from
343 the meander, Patel et al., 2019). Therefore, the ratio between rotational speed and translational
344 speed was > 5 for the entire lifetime of the eddy, suggesting that this eddy was highly nonlinear,
345 with a strong trapping power (Chelton et al., 2011).
346
347
348 Eddy trapping has significant consequences for the transport of salt and heat across the Antarctic
349 Circumpolar Current (Patel et al., 2019), impacts the distribution of primary producers (Dawson
350 et al., 2018; Frenger et al., 2018), weather (Frenger et al., 2013), and regulates the exchanges of
351 carbon crucial for climate (Moreau et al., 2017, Dufour et al, 2015). Our results show that eddy
352 trapping also impacts mesopelagic micronekton. It is difficult to evaluate whether micronekton
353 alone were trapped and transported or if it was their zooplanktonic prey that was transported and
354 the micronekton followed. Without complementary observations of zooplankton and
355 micronekton community composition, it is not possible to provide a definitive answer to this
356 question. However, two lines of evidence suggest that micronekton itself was trapped and
357 transported. First, studies focused on trawl and predator avoidance suggest that most
358 mesopelagic micronekton are generally lethargic when not vertically migrating or actively
359 escaping from a threat (Kaartvedt et al., 2012). Second, to initiate movement, it is likely that
360 micronekton would be responding to a stimulus, such as a gradient in temperature, pressure or
361 light (Franks, 1992). From the inner core of a mesoscale eddy, the closest horizontal gradients in
362 such properties (orders of magnitude weaker than the vertical ones) are tens of kilometers away
363 requiring for a mesopelagic fish to be able to perceive a gradient on scales that are four orders of
364 magnitudes larger than their body size.
365
366 Our results also indicate that, while the eddy core preserved many of the acoustical properties of
367 the PFZ, the structure of DSL in the eddy periphery was more similar to the SAZ. We can
368 interpret this pattern as an indicator of exchanges and mixing of water parcels (and the organisms
369 there contained) between the SAZ and the periphery of the eddy. This result is supported by the
370 analysis of water masses conducted using CTD data collected during the same voyage (Moreau
371 et al., 2017) and by the overall distribution of biogeochemical tracers (Patel et al., 2020)
372 including oxygen (Fig. S7). These findings are consistent with the theoretical results about eddy
373 trapping by Early et al. (2011), who highlighted that while eddy core waters can be ``isolated''
374 for a significant part of an eddy lifetime, the peripheries of eddies regularly exchange water
375 masses with the surroundings.
376
377 The strong difference between the SAZ and PFZ observed during INV2016_V02, both in terms
378 of integrated NASC, and distribution of DSL, was corroborated by the historical data from the
379 IMOS database, that consistently show less acoustic backscattering in the PFZ compared to the
380 SAZ. This was also shown in other studies that have found a general decrease in acoustic
381 backscattering with increased latitude (Escobar-Flores et al., 2018; Dornan et al., 2019).
382
383 The depth of DSL located at ~ 100m matches the mixed layer depth and the beginning of the
384 thermocline as well as a peak in the vertical distribution of ammonia that can reflect excretion by

385 marine organism such as zooplankton and fish (Patel et al., 2019). While changes in density
386 associated with the upper thermocline have been observed with 18 kHz echo-sounding (Stranne
387 et al., 2018), the high values of acoustic backscattering associated with this DSL are spread over
388 a depth range of more than 50m suggesting that they are more likely associated with a biological
389 signal.
390
391 Acoustic backscattering is commonly used as a fisheries-independent way to estimate fish
392 biomass (Fernandes et al., 2002; Kloser et al., 2009; Irigoien et al., 2014). Our main conclusion
393 is that the sampled cyclonic eddy had lower mesopelagic micronekton biomass compared to the
394 ambient SAZ waters and similarly to its origin on the PFZ. However, we should consider
395 alternative explanations for our observations. A recent study by Dornan et al., (2019) showed
396 that fish biomass estimated with acoustic backscattering decreased with increasing latitude in the
397 Southern Ocean, whereas biomass measured using mid-water trawls did not. This trend was
398 attributed to size and physiological temperature-driven changes in the resonating swim-bladders
399 that are responsible of strong backscattering signal. We think it is unlikely that the small
400 temperature and latitude difference between the eddy location in the SAZ and its SAF origin are
401 responsible for the observed differences. Another possibility is a change in community
402 composition of the micronekton: some species of micronekton do not have a swim-bladder or it
403 is filled with oil instead of air, causing weaker backscattering signals. This may have impacted
404 our results if the community composition was different in the SAZ compared to the SAF, but this
405 is part of our point: the eddy transported the community from its origin to where we sampled it.
406 Finally, fish belonging to the same species, but characterized by different size (and therefore of a
407 larger or smaller swim bladder) can backscatter sound differently producing different profiles of
408 acoustic backscattering (Fielding et al., 2012). During the IN2016_V02 expedition, we did not
409 carry out any mid-water trawling, and, therefore, we cannot discriminate further all aspects of
410 these hypotheses. However, our results suggest a difference between an eddy and the
411 surrounding waters in terms of biomass, community composition and/or physiological state.
412 Future studies will be needed to understand how these effects intertwine with each other and
413 affect the patchiness of micronekton distribution, eventually impacting the foraging strategies of
414 top predators.
415
416 Differences in the horizontal and vertical distribution of mesopelagic micronekton can have
417 important consequences for upper trophic levels. In the region of interest, the organisms
418 inhabiting the DSL we detected typically include myctophids, squids, swarming euphasiids, and
419 amphipods (Flynn and Kloser, 2012). These animals constitute the prey of a variety of marine
420 megafauna, including seabirds, penguins, and marine mammals (Cherel et al., 2010; Watanuki
421 and Thiebot, 2018; McMahon et al., 2019). For these diving predators, horizontal patchiness of
422 their prey field is an important driver of their foraging strategies, so differences in micronekton
423 composition or abundance can underpin their interactions with the prey fields which are in turn
424 set by the dynamics associated with mesoscale eddies. Furthermore, the differences in vertical
425 distribution of DSL are likely to have an impact on the accessibility of the prey to diving
426 predators. This difference might be particularly dramatic for air-breathing animals such as
427 seabirds and marine mammals whose foraging time underwater is limited by the need to breathe
428 at the surface (Jaud et al., 2012; Guinet et al., 2014; O'Toole et al., 2017), but also to fish whose
429 thermal niche can limit the vertical extent of their diving behavior (Gaube et al., 2018; Braun et
430 al., 2019). In general, the metabolic cost associated with getting the same amount of energy if the

431 prey is located deeper in the water column (and therefore potentially in colder water) will be
432 higher. These costs have the potential to result in cyclonic eddies, like the one we sampled, being
433 a non-profitable region for foraging.

434

References

452 Aksnes, D. L., Røstad, A., Kaartvedt, S., Martinez, U., Duarte, C. M., & Irigoien, X. (2017).
453 Light penetration structures the deep acoustic scattering layers in the global ocean. *Science*
454 *advances*, *3*(5), e1602468. https://doi.org/10.1126/sciadv.1602468

456 Belcher, A., Saunders, R.A., Tarling, G.A., 2019. Respiration rates and active carbon flux of
457 mesopelagic fishes (Family Myctophidae) in the Scotia Sea, Southern Ocean. Marine Ecology
458 Progress Series 610, 149–162. https://doi.org/10.3354/meps12861

460 Bianchi, D., Stock, C., Galbraith, E. D., & Sarmiento, J. L. (2013). Diel vertical migration:
461 Ecological controls and impacts on the biological pump in a one-dimensional ocean model.
462 *Global Biogeochemical Cycles*, *27*(2), 478-491. https://doi.org/10.1002/gbc.20031

464 Bianchi, D., & Mislan, K. A. S. (2016). Global patterns of diel vertical migration times and
465 velocities from acoustic data. *Limnology and Oceanography*, *61*(1), 353-364.
466 https://doi.org/10.1002/lno.10219

468 Bailleul, F., Cotté, C., & Guinet, C. (2010). Mesoscale eddies as foraging area of a deep-diving
469 predator, the southern elephant seal. *Marine Ecology Progress Series*, *408*, 251-264.
470 https://doi.org/10.3354/meps08560

472 Béhagle, N., Cotté, C., Lebourges-Dhaussy, A., Roudaut, G., Duhamel, G., Brehmer, P., ... &
473 Cherel, Y. (2017). Acoustic distribution of discriminated micronektonic organisms from a bi-

474   frequency processing: the case study of eastern Kerguelen oceanic waters. *Progress in*
475   *Oceanography*, *156*, 276-289. https://doi.org/10.1016/j.pocean.2017.06.004
476
477   Bodholt, H., 2002, June. The effect of water temperature and salinity on echo sounder
478   measurements. In *ICES Symposium on Acoustics in Fisheries* (pp. 1-7).
479
480   Bost, C. A., Cotté, C., Bailleul, F., Cherel, Y., Charrassin, J. B., Guinet, C., ... & Weimerskirch,
481   H. (2009). The importance of oceanographic fronts to marine birds and mammals of the southern
482   oceans. *Journal of Marine Systems*, *78*(3), 363-376.
483   https://doi.org/10.1016/j.jmarsys.2008.11.022
484
485   Boyd, S. H., Wiebe, P. H., Backus, R. H., Craddock, J. E., & Daher, M. A. (1986). Biomass of
486   the micronekton in Gulf Stream ring 82-B and environs: changes with time. *Deep Sea Research*
487   *Part A. Oceanographic Research Papers*, *33*(11-12), 1885-1905. https://doi.org/ 10.1016/0198-
488   0149(86)90084-1
489
490   Braun, C. D., Gaube, P., Sinclair-Taylor, T. H., Skomal, G. B., & Thorrold, S. R. (2019).
491   Mesoscale eddies release pelagic sharks from thermal constraints to foraging in the ocean
492   twilight zone. *Proceedings of the National Academy of Sciences*, *116*(35), 17187-17192.
493   https://doi.org/10.1073/pnas.1903067116
494
495   Chapman, C. C., Lea, M. A., Meyer, A., Sallée, J. B., & Hindell, M. (2020). Defining Southern
496   Ocean fronts and their influence on biological and physical processes in a changing climate.
497   *Nature Climate Change*, 1-11. https://doi.org/10.1038/s41558-020-0705-4
498
499   Chelton, D.B., Schlax, M.G. and Samelson, R.M., 2011. Global observations of nonlinear
500   mesoscale eddies. *Progress in oceanography*, *91*(2), pp.167-216.
501   https://doi.org/10.1016/j.pocean.2011.01.002
502
503   Cherel, Y., Fontaine, C., Richard, P., & Labatc, J. P. (2010). Isotopic niches and trophic levels of
504   myctophid fishes and their predators in the Southern Ocean. *Limnology and oceanography*,
505   *55*(1), 324-332. https://doi.org/10.4319/lo.2010.55.1.0324
506
507   Cotté, C., Park, Y. H., Guinet, C., & Bost, C. A. (2007). Movements of foraging king penguins
508   through marine mesoscale eddies. *Proceedings of the Royal Society B: Biological Sciences*,
509   *274*(1624), 2385-2391. https://doi.org/10.1098/rspb.2007.0775
510
511   Cotté, C., d'Ovidio, F., Dragon, A. C., Guinet, C., & Lévy, M. (2015). Flexible preference of
512   southern elephant seals for distinct mesoscale features within the Antarctic Circumpolar Current.
513   *Progress in Oceanography*, *131*, 46-58. https://doi.org/10.1016/j.pocean.2014.11.011
514
515   Craddock, J. E., Backus, R. H., & Daher, M. A. (1992). Vertical distribution and species
516   composition of midwater fishes in warm-core Gulf Stream meander/ring 82-H. *Deep Sea*
517   *Research Part A. Oceanographic Research Papers*, *39*, S203-S218.
518   https://doi.org/10.1016/S0198-0149(11)80012-9
519

Cuvier, G. *Le Règne Animal distribué d'après son Organisation pour à l'Histoire Naturelle des Animaux et d'Introduction à l'Anatomie Compare* (Deterville, 1817).

d'Ovidio, F., De Monte, S., Della Penna, A., Cotté, C., & Guinet, C. (2013). Ecological implications of eddy retention in the open ocean: a Lagrangian approach. *Journal of Physics A: Mathematical and Theoretical*, *46*(25), 254023. https://doi.org/ 10.1088/1751-8113/46/25/254023

Davison, P.C., Checkley, D.M., Koslow, J.A., Barlow, J., 2013. Carbon export mediated by mesopelagic fishes in the northeast Pacific Ocean. Progress in Oceanography 116, 14–30. https://doi.org/10.1016/j.pocean.2013.05.013

Dawson, H. R., Strutton, P. G., & Gaube, P. (2018). The unusual surface chlorophyll signatures of Southern Ocean eddies. *Journal of Geophysical Research: Oceans*, *123*(9), 6053-6069. https://doi.org/10.1029/2017JC013628

De Robertis, A., Bassett, C., Andersen, L.N., Wangen, I., Furnish, S. and Levine, M., 2019. Amplifier linearity accounts for discrepancies in echo-integration measurements from two widely used echosounders. *ICES Journal of Marine Science*, *76*(6), pp.1882-1892. https://doi.org/10.1093/icesjms/fsz040

Della Penna, A., De Monte, S., Kestenare, E., Guinet, C., & d'Ovidio, F. (2015). Quasi-planktonic behavior of foraging top marine predators. *Scientific reports*, *5*(1), 1-10. https://doi.org/10.1038/srep18063

Della Penna, A., Gaube, P., (2020). Mesoscale eddies structure mesopelagic communities. *Frontiers in Marine Science* https://doi.org/10.3389/fmars.2020.00454

Devine, B., Fennell, S., Themelis, D. and Fisher, J.A., (2021). Influence of anticyclonic, warm-core eddies on mesopelagic fish assemblages in the Northwest Atlantic Ocean. *Deep Sea Research Part I: Oceanographic Research Papers*, p.103555. http://doi.org/*10.1016/j.dsr.2021.103555*

Dornan, T., Fielding, S., Saunders, R. A., & Genner, M. J. (2019). Swimbladder morphology masks Southern Ocean mesopelagic fish biomass. *Proceedings of the Royal Society B*, *286*(1903), 20190353. https://doi.org/10.1098/rspb.2019.0353

Dragon, A. C., Monestiez, P., Bar-Hen, A., & Guinet, C. (2010). Linking foraging behaviour to physical oceanographic structures: Southern elephant seals and mesoscale eddies east of Kerguelen Islands. *Progress in Oceanography*, *87*(1-4), 61-71. https://doi.org/10.1016/j.pocean.2010.09.025

Dufour, C. O., Griffies, S. M., de Souza, G. F., Frenger, I., Morrison, A. K., Palter, J. B., ... & Slater, R. D. (2015). Role of mesoscale eddies in cross-frontal transport of heat and biogeochemical tracers in the Southern Ocean. *Journal of Physical Oceanography*, *45*(12), 3057-3081. https://doi.org/10.1175/JPO-D-14-0240.1

566

567 Early, J. J., Samelson, R. M., & Chelton, D. B. (2011). The evolution and propagation of
568 quasigeostrophic ocean eddies. *Journal of Physical Oceanography*, *41*(8), 1535-1555.
569 https://doi.org/10.1175/2011JPO4601.1

570

571 Escobar-Flores, P. C., Driscoll, R. L., & Montgomery, J. C. (2018). Spatial and temporal
572 distribution patterns of acoustic backscatter in the New Zealand sector of the Southern Ocean.
573 *Marine Ecology Progress Series*, *592*, 19-35. https://doi.org/10.3354/meps12489

574

575 Fennell, S., & Rose, G. (2015). Oceanographic influences on deep scattering layers across the
576 North Atlantic. *Deep Sea Research Part I: Oceanographic Research Papers*, *105*, 132-141.
577 https://doi.org/10.1016/j.dsr.2015.09.002

578

579 Fernandes, P. G., Gerlotto, F., Holliday, D. V., Nakken, O., & Simmonds, E. J. (2002). Acoustic
580 applications in fisheries science: the ICES contribution. ICES.

581

582 Fielding, S., Watkins, J. L., Collins, M. A., Enderlein, P., & Venables, H. J. (2012). Acoustic
583 determination of the distribution of fish and krill across the Scotia Sea in spring 2006, summer
584 2008 and autumn 2009. *Deep Sea Research Part II: Topical Studies in Oceanography*, *59*, 173-
585 188. https://doi.org/10.1016/j.dsr2.2011.08.002

586

587 Flynn, A. J., & Kloser, R. J. (2012). Cross-basin heterogeneity in lanternfish (family
588 Myctophidae) assemblages and isotopic niches (δ13C and δ15N) in the southern Tasman Sea
589 abyssal basin. *Deep Sea Research Part I: Oceanographic Research Papers*, *69*, 113-127.
590 https://doi.org/10.1016/j.dsr.2012.07.007

591

592 Franks, P. J. (1992). Sink or swim: Accumulation of biomass at fronts. *Marine ecology progress
593 series. Oldendorf*, *82*(1), 1-12. https://doi.org/10.3354/meps082001

594

595 Frenger, I., Gruber, N., Knutti, R., & Münnich, M. (2013). Imprint of Southern Ocean eddies on
596 winds, clouds and rainfall. *Nature geoscience*, *6*(8), 608-612. https://doi.org/10.1038/ngeo1863

597

598 Frenger, I., Münnich, M., & Gruber, N. (2018). Imprint of Southern Ocean eddies on
599 chlorophyll. *Biogeosciences (BG)*, *15*, 4781-4798. https://doi.org/10.5194/bg-15-4781-2018

600

601 Gaube, P., Braun, C. D., Lawson, G. L., McGillicuddy, D. J., Della Penna, A., Skomal, G. B., ...
602 & Thorrold, S. R. (2018). Mesoscale eddies influence the movements of mature female white
603 sharks in the Gulf Stream and Sargasso Sea. *Scientific reports*, *8*(1), 1-8.
604 https://doi.org/10.1038/s41598-018-25565-8

605

606 Godø, O. R., Samuelsen, A., Macaulay, G. J., Patel, R., Hjøllo, S. S., Horne, J., ... &
607 Johannessen, J. A. (2012). Mesoscale eddies are oases for higher trophic marine life. *PloS one*,
608 *7*(1). https://doi.org/10.1371/journal.pone.0030161

609

Greene, C. H., & Wiebe, P. H. (1990). Bioacoustical oceanography: new tools for zooplankton and micronekton research in the 1990s. *Oceanography*, *3*(1), 12-17. https://doi.org/10.5670/oceanog.1990.15

Guinet, C., Vacquié-Garcia, J., Picard, B., Bessigneul, G., Lebras, Y., Dragon, A. C., ... & Bailleul, F. (2014). Southern elephant seal foraging success in relation to temperature and light conditions: insight into prey distribution. *Marine Ecology Progress Series*, *499*, 285-301. https://doi.org/10.3354/meps10660

Hays, G. C. (2003). A review of the adaptive significance and ecosystem consequences of zooplankton diel vertical migrations. In *Migrations and Dispersal of Marine Organisms* (pp. 163-170). Springer, Dordrecht. https://doi.org/10.1023/B:HYDR.0000008476.23617.b0

Irigoien, X., Klevjer, T. A., Røstad, A., Martinez, U., Boyra, G., Acuña, J. L., ... & Agusti, S. (2014). Large mesopelagic fishes biomass and trophic efficiency in the open ocean. *Nature communications*, *5*(1), 1-10. https://doi.org/10.1038/ncomms4271

Jaud, T., Dragon, A. C., Garcia, J. V., & Guinet, C. (2012). Relationship between chlorophyll a concentration, light attenuation and diving depth of the southern elephant seal Mirounga leonina. *PLoS one*, *7*(10). https://doi.org/10.1371/journal.pone.0047444

Kaartvedt, S., Staby, A., & Aksnes, D. L. (2012). Efficient trawl avoidance by mesopelagic fishes causes large underestimation of their biomass. *Marine Ecology Progress Series*, *456*, 1-6. https://doi.org/10.3354/meps09785 https://doi.org/10.3354/meps09785

Klevjer, T. A., Irigoien, X., Røstad, A., Fraile-Nuez, E., Benítez-Barrios, V. M., & Kaartvedt, S. (2016). Large scale patterns in vertical distribution and behaviour of mesopelagic scattering layers. *Scientific reports*, *6*, 19873. https://doi.org/10.1038/srep19873

Kloser, R. J., Ryan, T. E., Young, J. W., & Lewis, M. E. (2009). Acoustic observations of micronekton fish on the scale of an ocean basin: potential and challenges. *ICES Journal of Marine Science*, *66*(6), 998-1006. https://doi.org/10.1093/icesjms/fsp077

Kloser, R. J., Ryan, T. E., Keith, G., & Gershwin, L. (2016). Deep-scattering layer, gas-bladder density, and size estimates using a two-frequency acoustic and optical probe. *ICES Journal of Marine Science*, *73*(8), 2037-2048. https://doi.org/10.1093/icesjms/fsv257

Kunnath, Haris., Kloser, R.J., Ryan, T.E., Downie, R.A., Keith, G. and Nau, A.W., 2021. Sounding out life in the deep using acoustic data from ships of opportunity. *Scientific Data*, *8*(1), pp.1-23. https://doi.org/10.1038/s41597-020-00785-8

Ladroit, Y., Escobar-Flores, P. C., Schimel, A. C., & O'Driscoll, R. L. (2020). ESP3: An open-source software for the quantitative processing of hydro-acoustic data. *SoftwareX*, *12*, 100581. https://doi.org/10.1016/j.softx.2020.100581

655 MacLennan, D. N., Fernandes, P. G., & Dalen, J. (2002). A consistent approach to definitions
656 and symbols in fisheries acoustics. *ICES Journal of Marine Science*, *59*(2), 365-369.
657 https://doi.org/10.1006/jmsc.2001.1158
658
659 McMahon, C. R., Hindell, M. A., Charrassin, J. B., Corney, S., Guinet, C., Harcourt, R., ... &
660 Bestley, S. (2019). Finding mesopelagic prey in a changing Southern Ocean. *Scientific Reports*,
661 *9*(1), 1-11. https://doi.org/10.1038/s41598-019-55152-4
662
663 Meeus, Jean H. Astronomical algorithms. Willmann-Bell, Incorporated, 1991.
664
665 Moreau, S., Della Penna, A., Llort, J., Patel, R., Langlais, C., Boyd, P. W., ... & Lenton, A.
666 (2017). Eddy-induced carbon transport across the Antarctic Circumpolar Current. *Global
667 Biogeochemical Cycles*, *31*(9), 1368-1386. https://doi.org/10.1002/2017GB005669
668
669 Morrow, R., Donguy, J. R., Chaigneau, A., & Rintoul, S. R. (2004). Cold-core anomalies at the
670 subantarctic front, south of Tasmania. *Deep Sea Research Part I: Oceanographic Research
671 Papers*, *51*(11), 1417-1440. https://doi.org/10.1016/j.dsr.2004.07.005
672
673 Murphy, E. J., Cavanagh, R. D., Drinkwater, K. F., Grant, S. M., Heymans, J. J., Hofmann, E. E.,
674 ... & Johnston, N. M. (2016). Understanding the structure and functioning of polar pelagic
675 ecosystems to predict the impacts of change. *Proceedings of the Royal Society B: Biological
676 Sciences*, *283*(1844), 20161646. https://doi.org/10.1098/rspb.2016.1646
677
678 Nelson, D.M. and Smith Jr, W.0., 1991. Sverdrup revisited: Critical depths, maximum
679 chlorophyll levels, and the control of Southern Ocean productivity by the irradiance-mixing
680 regime. *Limnology and Oceanography*, *36*(8), pp.1650-1661.
681 https://doi.org/10.4319/lo.1991.36.8.1650
682
683 Orselli, I.B., Kerr, R., de Azevedo, J.L., Galdino, F., Araujo, M. and Garcia, C.A., 2019. The
684 sea-air CO2 net fluxes in the South Atlantic Ocean and the role played by Agulhas eddies.
685 *Progress in Oceanography*, *170*, pp.40-52. https://doi.org/10.1016/j.pocean.2018.10.006
686
687 O'Toole, M., Guinet, C., Lea, M. A., & Hindell, M. A. (2017). Marine predators and
688 phytoplankton: how elephant seals use the recurrent Kerguelen plume. *Marine Ecology Progress
689 Series*, *581*, 215-227. https://doi.org/10.3354/meps12312
690
691 Patel, R. S., Phillips, H. E., Strutton, P. G., Lenton, A., & Llort, J. (2019). Meridional Heat and
692 Salt Transport Across the Subantarctic Front by Cold-Core Eddies. *Journal of Geophysical
693 Research: Oceans*, *124*(2), 981-1004. https://doi.org/10.1029/2018JC014655
694
695 Patel, R. S., Llort, J., Strutton, P. G., Phillips, H. E., Moreau, S., Conde Pardo, P., & Lenton, A.
696 The biogeochemical structure of Southern Ocean mesoscale eddies. *Journal of Geophysical
697 Research: Oceans*, e2020JC016115. https://doi.org/10.1029/2020JC016115
698
699 Proud, R., Cox, M. J., & Brierley, A. S. (2017). Biogeography of the global ocean's mesopelagic
700 zone. *Current Biology*, *27*(1), 113-119. https://doi.org/10.1016/j.cub.2016.11.003

Rohr, T., Harrison, C., Long, M. C., Gaube, P., & Doney, S. C. The simulated biological response to Southern Ocean eddies via biological rate modification and physical transport. *Global Biogeochemical Cycles*, e2019GB006385. https://doi.org/10.1029/2019GB006385

Rohr, T., Harrison, C., Long, M. C., Gaube, P., & Doney, S. C. Eddy-modified iron, light, and phytoplankton cell division rates in the simulated Southern Ocean. *Global Biogeochemical Cycles*, e2019GB006380. https://doi.org/10.1029/2019GB006380

Røstad, A., Kaartvedt, S., & Aksnes, D. L. (2016). Light comfort zones of mesopelagic acoustic scattering layers in two contrasting optical environments. *Deep Sea Research Part I: Oceanographic Research Papers*, *113*, 1-6. https://doi.org/10.1016/j.dsr.2016.02.020

Ryan, T. E., Kloser, R. J., & Macaulay, G. J. (2009). Measurement and visual verification of fish target strength using an acoustic-optical system attached to a trawlnet. *ICES Journal of Marine Science*, *66*(6), 1238-1244. https://doi.org/10.1093/icesjms/fsp122

Ryan, T. (2011). Overview of data collection, management and processing procedures of underway acoustic data. IMOS BASOOP sub-facility.

Son, S., & Wang, M. (2015). Diffuse attenuation coefficient of the photosynthetically available radiation Kd (PAR) for global open ocean and coastal waters. *Remote Sensing of Environment*, *159*, 250-258. https://doi.org/10.1016/j.rse.2014.12.011

Subramaniam, R. C., Corney, S. P., Swadling, K. M., & Melbourne-Thomas, J. (2020). Exploring ecosystem structure and function of the northern Kerguelen Plateau using a mass-balanced food web model. *Deep Sea Research Part II: Topical Studies in Oceanography*, 104787. https://doi.org/10.1016/j.dsr2.2020.104787

Stranne, C., Mayer, L., Jakobsson, M., Weidner, E., Jerram, K., Weber, T.C., Anderson, L.G., Nilsson, J., Björk, G. and Gårdfeldt, K., 2018. Acoustic mapping of mixed layer depth. *Ocean Science*, *14*(3), pp.503-514 https://doi.org/10.5194/os-14-503-2018

Tew-Kai, E., Rossi, V., Sudre, J., Weimerskirch, H., Lopez, C., Hernandez-Garcia, E., ... & Garçon, V. (2009). Top marine predators track Lagrangian coherent structures. *Proceedings of the National Academy of Sciences*, *106*(20), 8245-8250. https://doi.org/10.1073/pnas.0811034106

Urmy, S. S., & Horne, J. K. (2016). Multi-scale responses of scattering layers to environmental variability in Monterey Bay, California. *Deep Sea Research Part I: Oceanographic Research Papers*, *113*, 22-32. https://doi.org/ 10.1016/j.dsr.2016.04.004

Watanuki, Y., & Thiebot, J. B. (2018). Factors affecting the importance of myctophids in the diet of the world's seabirds. *Marine Biology*, *165*(4), 79. https://doi.org/10.1007/s00227-018-3334-y

747   Wiebe, P. H., Morton, A. W., Bradley, A. M., Backus, R. H., Craddock, J. E., Barber, V., ... &
748   Flierl, G. D. 1. (1985). New development in the MOCNESS, an apparatus for sampling
749   zooplankton and micronekton. *Marine Biology*, *87*(3), 313-323.
750   https://doi.org/10.1007/BF00397811
751